Sub-Nyquist Medical Ultrasound Imaging:
En Route to Cloud Processing

Alon Eilam*, Tanya Chernyakova*, Yonina C. Eldar* and Arcady Kempinski**

*Department of Electrical Engineering, Technion, Israel Institute of Technology, Haifa, Israel

Email: aeilam@tx.technion.ac.il, ctanya@tx.technion.ac.il, yonina@ee.technion.ac.il

**GE Healthcare, Haifa, Israel

Email: arcady.kempinski@med.ge.com

Abstract—In medical ultrasound imaging, a pulse of known shape is transmitted into the respective medium, and the received echoes are sampled and digitally processed in a way referred to as beamforming to form an ultrasound image. Applied spatially, beamforming allows to improve resolution and signal-to-noise ratio. The structure of medical ultrasound signals allow for significant reduction of both sampling and processing rates by relying on ideas of Xampling, sub-Nyquist sampling and frequency domain beamforming. In this paper we present an implementation on an ultrasound machine using sub-Nyquist sampling and processing and the obtained imaging results. The provided system configuration exploits the advantages of beamforming in the frequency domain, which is performed at a low-rate. Our results prove that the concept of porting heavy computational tasks to the cloud is feasible for medical ultrasound, leading to potential of considerable reduction in future ultrasound machines size, power consumption and cost.

Index Terms—Array Processing, Ultrasound, Beamforming, Compressed Sensing, Sub-Nyquist

I. INTRODUCTION

Diagnostic ultrasound has been used for decades to visualize body structures. The overall imaging process is described as follows: An energy pulse is transmitted along a narrow beam. During its propagation echoes are scattered by acoustic impedance perturbations in the tissue, and detected by the elements of the transducer. Collected data are sampled and digitally processed in a way referred to as beamforming, which results in signal-to-noise ratio (SNR) enhancement. Such a beamformed signal forms a line in the image.

According to the classic Shannon-Nyquist theorem [1], the sampling rate at each transducer element should be at least twice the bandwidth of the detected signal. In legacy systems, rates up to 3-10 times the modulation frequency are required in order to avoid artifacts caused by digital implementation of beamforming in the time domain [2]. Such rates can be up to 4 times the Nyquist rate of the detected signal. Taking into account the number of transducer elements and the number of lines in an image, the amount of sampled data that needs to be digitally processed is enormous, motivating methods to reduce sampling rates.

Reduction of processing rate is possible within the classical sampling framework, by exploiting the fact that the signal is modulated onto a carrier and occupies only a portion of its entire baseband bandwidth. Accordingly, state-of-the-art systems digitally demodulate down-sample the data at the system's front-end. However, this does not change the sampling rate since demodulation takes place in the digital domain. In addition, resulting processing rate may be reduced up to $1/4$ of the standard beamforming rate, but the signal becomes complex in this setup, and the number of samples effectively is only twice smaller.

A different approach to sampling rate reduction was introduced in [3]. Tur et. al. regard the ultrasound signal detected by each receiver within the framework of finite rate of innovation (FRI) [4], modeling it as L replicas of a known pulse-shape, caused by scattering of the transmitted pulse from reflectors, located along the transmitted beam. Such an FRI signal is fully described by $2L$ parameters, corresponding to the replica's delays and amplitudes. These parameters can be extracted from a small set of the signal's Fourier series coefficients. A mechanism, referred to as Xampling, derived in [5], [6] extracts such a set of coefficients from $4L$ real-valued samples. This work is continued in [7], where Wagner et. al. introduce a generalized scheme, referred to as compressed beamforming, which allows to compute the Fourier series coefficients of the beamformed signal from the low-rate samples of signals detected at each element. The problem of reconstruction of the beamformed signal from a small number of its Fourier series coefficients is solved via a compressed sensing (CS) technique, while assuming a small number L of replicas. This approach allows to reconstruct an image comprised of macroscopic perturbations, but did not treat the speckle, which is of significant importance in medical imaging.

A solution to the problem of speckle retaining was proposed in [8], where Chernyakova et al. extended the notion of compressed beamforming to beamforming in frequency and proposed alternative approach for reconstruction of the signal from partial frequency data. Beamforming in frequency exploits the low bandwidth of the signal and allows to bypass the oversampling required for beamforming in time. Arbitrary set of discrete Fourier transform (DFT) coefficients of the beamformed signal can be computed as a linear combination of DFT coefficients of the detected signals. The latter can be computed from low-rate generalized samples of the detected signals, obtained by Xampling scheme. Once partial beamformed frequency data is obtained, appropriate CS techniques can be used to recover the beamformed signal. Such a framework, utilizing sub-Nyquist sampling, frequency domain beamforming and CS techniques for signal recovery allows for significant reduction in both sampling and processing rates, while retaining sufficient image quality.

In this paper we introduce the implementation of beamforming in frequency and sub-Nyquist processing on a stand alone ultrasound machine and show that such processing is feasible and is not just a theoretical framework. Low-rate processing is performed on the data obtained in real-time by scanning a phantom with an 64 element probe. The proposed approach allows for significant rate redaction with respect to the lowest processing rates that are achievable today. The achieved saving in data and processing rates enable beamforming by remote servers in a computer network cloud. This approach is expected to have a significant impact on system size, power consumption and cost. It consolidates with the trend of cloud computing in general [9] and its proposed application in medical ultrasound imaging systems [10].

II. BEAMFORMING IN TIME

We begin by describing the beamforming process which takes place in a typical B-mode imaging cycle. In the transmit path, a pulse is generated and transmitted by the array of transducer elements. The pulse transmitted by each element is timed and scaled, so that the superposition of all transmitted pulses creates a directional beam propagating at a certain angle. By subsequently transmitting at different angles, a whole sector is radiated. The real time computational complexity in the transmit path is negligible since transmit parameters per angle are calculated off-line and saved in tables.

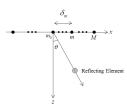Consider an array comprised of M transceiver elements aligned along the x axis, as illustrated in Fig. 1.

Fig. 1: M transceivers aligned along the x axis, with an acoustic pulse transmitted at direction θ.

The reference element m_0 is set at the origin and the distance to the m-th element is denoted by δ_m. The image cycle begins at $t = 0$, when the array transmits an energy pulse in the direction θ. After each transmission, the transducer array immediately switches to receive mode. The pulse propagates trough the tissue at speed c, and at time $t \geq 0$ its coordinates are $(x, z) = (ct \sin \theta, ct \cos \theta)$. A potential point reflector located at this position scatters the energy, such that the echo is detected by all array elements at a time depending on their locations. Denote by $\varphi_m(t; \theta)$ the signal detected by the m-th element and by $\hat{\tau}_m(t; \theta)$ the time of detection. It is readily seen that:

$$\hat{\tau}_m(t; \theta) = t + \frac{d_m(t; \theta)}{c}, \qquad (1)$$

where $d_m(t; \theta) = \sqrt{(ct \cos \theta)^2 + (\delta_m - ct \sin \theta)^2}$ is the distance traveled by the reflection. Beamforming involves averaging the signals detected by multiple receivers while compensating the differences in detection time.

Using (1), the detection time at m_0 is $\hat{\tau}_{m_0}(t; \theta) = 2t$ since $\delta_{m_0} = 0$. Applying an appropriate delay to $\varphi_m(t; \theta)$, such that the resulting signal $\hat{\varphi}_m(t; \theta)$ satisfies $\hat{\varphi}_m(2t; \theta) = \varphi_m(\hat{\tau}_m(t; \theta))$, we can align the reflection detected by the m-th receiver with the one detected at m_0. Denoting $\tau_m(t; \theta) = \hat{\tau}_m(t/2; \theta)$ and using (1), the following aligned signal is obtained:

$$\hat{\varphi}_m(t; \theta) = \varphi_m(\tau_m(t; \theta); \theta), \qquad (2)$$
$$\tau_m(t; \theta) = \frac{1}{2} \left(t + \sqrt{t^2 - 4(\delta_m/c)t \sin \theta + 4(\delta_m/c)^2} \right).$$

The beamformed signal may now be derived by averaging the aligned signals:

$$\Phi(t; \theta) = \frac{1}{M} \sum_{m=1}^{M} \hat{\varphi}_m(t; \theta). \qquad (3)$$

Such a beamformed signal is optimally focused at each depth and hence exhibits improved angular localization and enhanced SNR.

Ultrasound systems perform the beamforming process defined in (3) in the digital domain: analog signals $\varphi_m(t; \theta)$ are amplified and sampled by an Analog to Digital Converter (ADC), preceded by an anti-aliasing filter. As mentioned in Section I, in legacy

systems severe oversampling is required in order to perform beamforming digitally. State-of-the-art systems, though, exploit the fact that the detected signals are centered about a carrier frequency f_0. As provided in [11] this signal can be represented in the form $\varphi_m(t; \theta) = i_m(t; \theta)(\cos \omega_0 t) + q_m(t; \theta)(\sin \omega_0 t)$ where $i_m(t; \theta)$ and $q_m(t; \theta)$ are its in-phase and quadrature components. Each quadrature component bandwidth is identical to that of the transmitted pulse bandwidth.

The demodulation process is performed digitally since digital demodulation eliminates the analog mixers required in [11]. Fig. 2 presents a schematic block diagram of the transmit and receive front-end of a state-of-the-art medical ultrasound system. The drawback of digital demodulation is a requirement for high sampling rates of the analog amplifier output. We note that in state-of-the-art systems this rate can be as high as 50 MHz. Following demodulation, low pass filters are used for decimation. This operation provides reduction in processing rate, which is now dictated by the quadrature signals bandwidth. The sampled signals are scaled, time delayed summed and averaged according to (3).

The beamforming process is repeated for multiple angles until a whole sector is covered. Computation wise, this is the weakest link of the receive path, limiting the achievable image frame rate. To provide enough computational resources, most systems use dedicated DSP engines, with considerable impact on system's size, power consumption and cost.

To get a sense of rate requirements in medical ultrasound, we evaluate the number of samples taken at each transducer element. In our study we used a breadboard ultrasonic scanner of 64 acquisition channels, similar to the one depicted in Fig. 2. The radiated depth $r = 15.7$ cm and the speed of sound $c = 1540$ m/sec yield a signal of duration $T = 2r/c \simeq 204$ μsec. The acquired signal is characterized by a narrow bandpass bandwidth of 1.77 MHz, centered at the carrier frequency $f_0 \approx 3.4$ MHz, leading, theoretically, to a standard beamforming rate of $f_b \approx 12$ MHz and $T f_b = 2448$ real-valued samples. In practice, the imaging system samples the detected signals at rate of 50 MHz and then digitally demodulates and down-samples it to demodulated processing rate of $f_p \approx 2.94$ MHz, resulting in 1224 real-valued samples per transducer element. Multiplying the number of real-valued samples by the number of array elements and resolution of 12 bits per sample we get a data rate of 0.95 MBit/beam. Since acquiring at about 100 different angles is required in order to create a single image, the data rate per frame is 95 Mbit/frame. For moving images at rate 25 frames/sec, the overall beamform sampling data rate would thus be above 2.33 Gbit/Sec.

To conclude this section, processing in the time domain even by state-of-the-art systems imposes high sampling rate and considerable burden on the beamforming block. This high data rate makes it infeasible to perform beamforming by a remote sever. We now show that the number of samples and processing rate can be reduced significantly by sub-Nyquist sampling, beamforming in frequency and CS-based signal reconstruction.

III. BEAMFORMING IN FREQUENCY

A. Beamforming in Frequency and Sampling Scheme

Beamforming in frequency introduced in [8] is an extension of the compressed beamforming framework, developed by Wagner et al. [7]. This technique allows to compute the DFT coefficients of the beamformed signal from a weighted average of the DFT coefficients
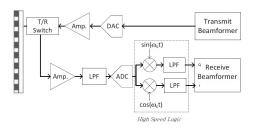
Fig. 2: Transmit and receive front-end of state-of-the-art medical ultrasound system.

of each individual signal:

$$c_k \simeq \frac{1}{M} \sum_{m=1}^{M} \sum_{n \in \nu(k)} \varphi_m[n] Q_{k,m;\theta}[k-n], \qquad (4)$$

where c_k and $\varphi_m[n]$ denote the DFT coefficients of the beamformed and individual signals respectively, $Q_{k,m;\theta}[n]$ are the Fourier coefficients of the distortion function $q_{k,m}(t;\theta)$, defined in [8].

It is important to emphasize that $\{Q_{k,m;\theta}[n]\}$ are defined by the geometry of the transducer and do not depend on the detected signals. Hence, these weights can be computed off-line and be used as a look-up-table during the imaging cycle. In addition, numerical studies show that most of the energy of the set $\{Q_{k,m;\theta}[n]\}$ is concentrated around the direct current (DC) component, implying small cardinality of the set $\nu(k)$. Therefore, in order to calculate an arbitrary set κ of DFT coefficients of the beamformed signal, we need $\nu = \cup_{k \in \kappa} \nu(k)$ DFT coefficients of each one of the individual signals. Experimental results show that due to the decay property of $\{Q_{k,m;\theta}[n]\}$, $|\nu| \approx |\kappa|$. Hence, the beamforming in frequency is performed at a low rate, dictated by the cardinality of set κ, and the sampling at each transducer element is reduced to extraction of $K = |\kappa|$ DFT coefficients of the detected signal.

To this end, similarly to [7] and [6], we can use a mechanism, referred to as Xampling, derived in [3]. Such Xampling scheme allows to obtain K coefficients from K point-wise samples of the detected signal filtered with an appropriate kernel $s^*(-t)$, which is designed according to the transmitted pulse-shape and the required set κ. Thus, the DFT coefficients can be computed from low-rate generalized samples of the signal. It is important to emphasize that processing rate in this case is twice the sampling rate, since K point-wise samples are real, but K coefficients are complex. To conclude, the number of samples that should be taken at each individual element is equal to the number of DFT coefficients of the beamformed signal we want to compute, leading to significant rate reduction.

B. Beamformed Signal Reconstruction

Next, we would like to address the following question: how can we reconstruct the beamformed signal from such partial frequency data? We begin by introducing the parametric model for the beamformed signal. According to [3], [7], the beamformed signal in ultrasound imaging obeys an FRI model:

$$\Phi(t;\theta) \simeq \sum_{l=1}^{L} \tilde{b}_l h(t-t_l), \qquad (5)$$

where $h(t)$ is the transmitted pulse, L is the number of scattering elements in direction θ, $\{\tilde{b}_l\}_{l=1}^{L}$ are the unknown amplitudes of the reflections and $\{t_l\}_{l=1}^{L}$ denote the unknown delays. The signal in (5) is completely defined by the unknown amplitudes and delays.

Since the beamformed signal only exists in the digital domain, we can rewrite this model accordingly by sampling both sides of (5) at rate f_s and quantizing the unknown delays $\{t_l\}_{l=1}^{L}$ with quantization step $1/f_s$, such that $t_l = q_l/f_s, q_l \in \mathbb{Z}$:

$$\Phi[n;\theta] \simeq \sum_{l=1}^{L} \tilde{b}_l h[n-q_l] = \sum_{l=0}^{N-1} b_l h[n-l], \qquad (6)$$

where
$$b_l = \begin{cases} \tilde{b}_l & \text{if } l = q_l \\ 0 & \text{otherwise.} \end{cases} \qquad (7)$$

Calculating the DFT using (6):

$$c_k = \sum_{n=0}^{N-1} \Phi[n;\theta] e^{-i\frac{2\pi}{N}kn} = h_k \sum_{l=0}^{N-1} b_l e^{-i\frac{2\pi}{N}kl}, \qquad (8)$$

where h_k is the DFT coefficient of $h[n]$. Assuming that we have a set κ, $|\kappa| = K$ of DFT coefficients of the beamformed signal, (8) can be recast in vector-matrix notation:

$$\mathbf{c} = \mathbf{HDb}, \qquad (9)$$

where $\mathbf{c}$ is a K-length vector with k-th entry c_k, $\mathbf{H}$ is a $K \times K$ diagonal matrix with h_k as its k-th entry, $\mathbf{D}$ is a $K \times N$ matrix formed by taking the set κ of rows from an $N \times N$ DFT matrix, and vector $\mathbf{b}$ is of length N with l-th entry b_l.

Our goal is to extract those values, namely the unknown vector $\mathbf{b}$, from the measurement vector $\mathbf{c}$ of DFT coefficients. This can be done by applying CS techniques. A typical beamformed ultrasound signal is comprised of a relatively small number of strong reflections, corresponding to strong perturbations in the tissue, and a bunch of much weaker scattered echoes, originated from microscopic changes in acoustic impedance of the tissue. Hence, it is natural to assume that coefficient vector $\mathbf{b}$ is compressible or approximately sparse. This approach can be translated into the l_1 optimization problem:

$$\min_{\mathbf{b}} \|\mathbf{b}\|_1 \quad \text{subject to} \quad \|\mathbf{HDb} - \mathbf{c}\|_2 \leq \varepsilon, \qquad (10)$$

which can be solved using numerous CS techniques.

To demonstrate beamforming in frequency and evaluate the impact of rate reduction on image quality, we applied the proposed method on in vivo cardiac data obtained by the imaging system, similar to one depicted in Section II. Due to slightly wider bandwidth of the transmitted pulse, standard beamforming rate in this case is $f_b = 16$ MHz, leading to 3360 real-valued samples. In practice, demodulated processing rate $f_p = 4$ MHz leads to 832 real-valued samples, used to perform beamforming in time. To perform beamforming in frequency we used a subset κ of 100 DFT coefficients, which can be obtained from 100 real-valued samples by the proposed Xampling scheme. This implies 32 fold reduction in sampling and 16 fold reduction in processing rate, compared to standard beamforming rate, as well as 8 fold reduction compared to demodulated processing rate. As can be seen in Fig. 3, we are able to retain sufficient image quality.

C. Implementation, System Configuration and Data Rates

As a next step we have implemented low-rate frequency domain beamforming on an ultrasound imaging system. The lab setup used for implementation and testing is shown in Fig. 4. We have used a state of the art ultrasound machine, a phantom and an ultrasound scanning probe with parameters identical to those presented in Section II. At this point of our work, as illustrated in Fig. 5, in-phase and quadrature components of the detected signals were used to obtain the desired set of their DFT coefficients.

Using this set, the DFT coefficients of beamformed signal were obtained using (4). In this setup sampling rate remained unchanged,
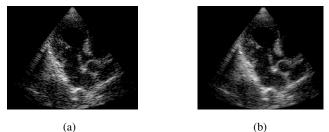
(a)   (b)

Fig. 3: Cardiac images obtained by (a) Beamforming in frequency at a low rate (b) Beamforming in time at a standard rate

(a)   (b)

Fig. 6: Phantom images obtained by (a) Beamforming in frequency at a low rate (b) Beamforming in time at a standard rate

but the frequency domain beamforming was performed at a low rate. In our experiments we computed 76 DFT coefficients of beamformed signal, using 76 DFT coefficients of each one of the detected signals. This corresponds to 152 real-valued samples used for beamforming in frequency. As mentioned in Section II, the number of samples required by standard beamforming rate is 2448 and the number of samples required by demodulated processing rate is 1224. Hence, beamforming in frequency is performed at the rate corresponding to $152/2448 \approx 1/16$ of standard beamforming rate and to $152/1224 \approx 1/8$ of demodulated processing rate. Images obtained by low-rate beamforming and frequency and standard time-domain beamforming are presented in Fig. 6. As can be readily seen, we are able to retain sufficient image quality despite the significant reduction in processing rate.

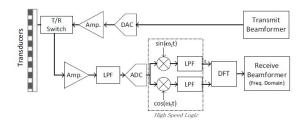Fig. 4: Lab setup: Ultrasound system, probe and cardiac phantom.

Fig. 5: Transmit and receive paths of medical ultrasound system with beamforming in the frequency domain.

D. Conclusions and Future Work

In this work we implemented a novel approach of frequency domain beamforming on a stand alone ultrasound machine. This framework allows for 8 fold reduction in processing rate with respect to the lowest processing rates that are achievable today. Rate
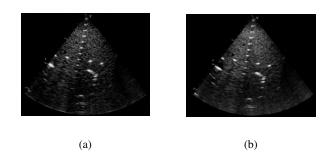
reduction with respect to standard beamforming rates is even higher. It is important to emphasize that the achieved rate is far below the Nyquist rate of the signal. It can be readily seen, that achieved beamforming data rate is about 290 MBit/sec, Vs. 2.33 GBit/sec in the state of the art system example of section II.

Our implementation was done on a state-of-the-art system, sampling the output of the analog amplifier at a high rate. Data and processing rates reduction took place following DFT, in the frequency domain. However, by implementing the Xampling scheme for sampling analog amplifier output as described in Section III-A, the required 76 DFT coefficients of the detected signals, required for frequency domain beamforming, can be obtained from 76 real-valued low rate samples. This implies achieving 32 fold reduction in signal sampling rate with respect to standard beamforming sampling rate.

By utilizing the low data rate, the beamformer can be either local or in a network cloud, providing for cloud based ultrasound imaging systems.

REFERENCES

[1] C. E. Shannon, "Communication in the presence of noise," *Proceedings of the IRE*, vol. 37, no. 1, pp. 10–21, 1949.
[2] T. L. Szabo, *Diagnostic Ultrasound Imaging: Inside Out*, Academic Press, 2004.
[3] R. Tur, Y. C. Eldar, and Z. Friedman, "Innovation rate sampling of pulse streams with application to ultrasound imaging," *IEEE Transactions on Signal Processing*, vol. 59, no. 4, pp. 1827–1842, 2011.
[4] M. Vetterli, P. Marziliano, and T. Blu, "Sampling signals with finite rate of innovation," *IEEE Transactions on Signal Processing*, vol. 50, no. 6, pp. 1417–1428, 2002.
[5] K. Gedalyahu, R. Tur, and Y. C. Eldar, "Multichannel sampling of pulse streams at the rate of innovation," *IEEE Transactions on Signal Processing*, vol. 59, no. 4, pp. 1491–1504, 2011.
[6] E. Baransky, G. Itzhak, I. Shmuel, N. Wagner, E. Shoshan, and Y. C. Eldar, "A sub-nyquist radar prototype: Hardware and algorithms," *submitted to IEEE Transactions on Aerospace and Electronic Systems, special issue on Compressed Sensing for Radar*, Aug. 2012.
[7] N. Wagner, Y. C. Eldar, and Z. Friedman, "Compressed beamforming in ultrasound imaging," *IEEE Transactions on Signal Processing*, vol. 60, no. 9, pp. 4643–4657, 2012.
[8] T. Chernyakova, Y. C. Eldar, and R. Amit, "Fourier domain beamforming for medical ultrasound," in *Acoustics, Speech and Signal Processing (ICASSP), 2013 IEEE International Conference on*. IEEE, 2013.
[9] I. Foster, Y. Zhao, I. Raicu, and S. Lu, "Cloud computing and grid computing 360-degree compared," in *Grid Computing Environments Workshop, 2008. GCE'08*. IEEE, 2008, pp. 1–10.
[10] A. Meir and B. Rubinsky, "Distributed network, wireless and cloud computing enabled 3-D ultrasound; a new medical technology paradigm," *PloS one*, vol. 4, no. 11, pp. e7974, 2009.
[11] J. E. Powers, D. J. Phillips, and M. Brandestini, "Ultrasound phased array delay lines based on quadrature sampling techniques," *IEEE Trans. Sonics and Ultrasonics*, vol. 27, no. 6, pp. 287–294, 1980.